

A Structurally Tunable DNA-Based Extracellular Matrix

Faisal A. Aldaye,^{*,†,‡} William T. Senapedis,[†] Pamela A. Silver,^{*,†,‡} and Jeffrey C. Way[‡]

Department of Systems Biology, Harvard Medical School, 200 Longwood Avenue, Boston, Massachusetts 02115, United States, and Wyss Institute for Biologically Inspired Engineering, Harvard University, 3 Blackfan Circle, Boston, Massachusetts 02115, United States

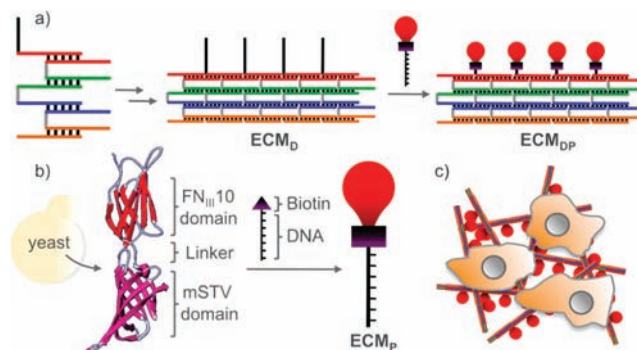
Received June 21, 2010; E-mail: faisal_aldaye@hms.harvard.edu; pamela_silver@hms.harvard.edu

Abstract: The principles of DNA nanotechnology and protein engineering have been combined to generate a new class of artificial extracellular matrices. The potential of this material for ex vivo cellular scaffolding was demonstrated using experiments in which human cervical cancer cells were found to adhere strongly, stay alive, and grow with high migration rates. The use of DNA in our DNA/protein-based matrices makes these structures inherently amenable to structural tunability. By engineering single-stranded domains into the DNA portions, we were able to fine-tune the scaffold's persistence length and stiffness as perceived by cells. This was used to direct the outcome of the cell's cytoskeletal arrangement and overall shape, the status of its signal transduction protein p-FAK, and the localization of its intracellular transcription factors FOXO1a. This contribution lays the groundwork for the facile and modular construction of programmable extracellular matrices that can bring about the systematic study and replication of the naturally occurring extracellular niche.

The construction of artificial matrices that mimic the structure and function of the naturally occurring extracellular matrix (ECM) is a central challenge for tissue engineering.¹ The difficulty lies in our inability to replicate the biophysical and chemical signaling effectors found in the ECM. Although polymeric hydrogels, nanofibrillar synthetic biomaterials, and poly(ethylene glycol)-based materials have been used for cell adhesion and proliferation,² there is a need for scaffolds that are structurally programmable. DNA nanotechnology uses base pairing to generate predefined one-, two-, and three-dimensional assemblies for templated growth of materials, organization of proteins and nanoparticles, and as platforms for diagnosis and delivery.³ Here we have combined the principles of DNA nanotechnology with protein engineering to generate a new class of DNA/protein extracellular matrices and demonstrated their potential for cell adhesion and growth. The use of DNA means that our assemblies are inherently amenable to structural programming, which we have demonstrated and used to fine-tune cell morphology, behavior, signaling, and transcription factor localization.

A DNA/protein-based matrix (**ECM_{DP}**) was constructed from a DNA ribbon (**ECM_D**) surface-functionalized with proteins (**ECM_P**) containing the RGD domain of human fibronectin. This protein was selected because of its role in cellular adhesion, survival, proliferation, and migration.⁴ The structure of **ECM_P** was inspired by collagen. It was assembled from five DNA strands that form a four-helix ribbon^{3d} with overhangs (Scheme 1a), and it was analyzed

Scheme 1



using atomic force microscopy (AFM) (Figure 1a).⁵ **ECM_P** was expressed in *Pichia pastoris* and contains an FN_{III}10 domain, a flexible (Gly₄Ser)₃ linker, a monomeric streptavidin domain for conjugation to 5'-biotin DNA, and a His₆ tag (Scheme 1b).⁵ The 1:1 binding of **ECM_P** with DNA was confirmed using gel-shift assays.⁵ Addition of **ECM_P** to **ECM_D** generated the DNA/protein matrix **ECM_{DP}** (Figure 2b).⁵

To study **ECM_{DP}**-promoted cell adhesion and migration, HeLa cervical cancer cells were used because of their well-characterized

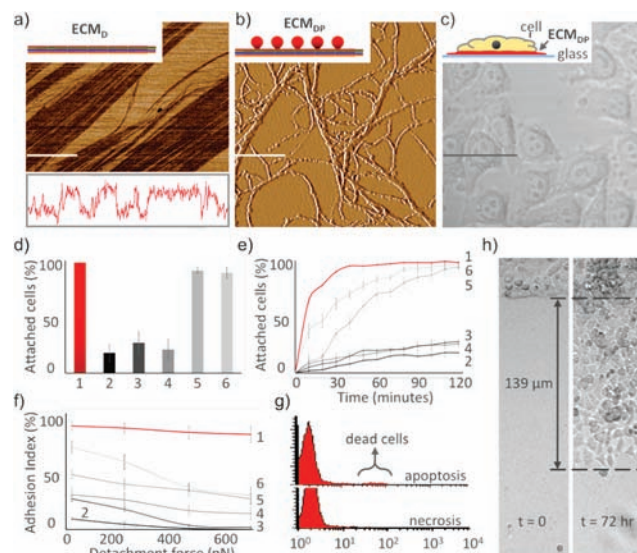


Figure 1. (a) AFM characterization of **ECM_D** with cross-sectional height analysis (lower panel). Scale bar = 10 μm. (b) AFM characterization of **ECM_{DP}**. Scale bar = 1 μm. (c) HeLa cells on **ECM_{DP}**-coated glass plates. Scale bar = 15 μm. (d) Percentages of cells that attached onto plates coated with (1) **ECM_{DP}**, (2) **ECM_P**, (3) **ECM_P**, (4) unconjugated **ECM_D** and **ECM_P**, (5) polylysine, and (6) fibronectin. (e) Rate of attachment. (f) Strength of attachment as a function of detachment force. (g) Viability of cells growing on **ECM_{DP}**. (h) Migration of HeLa cells growing on **ECM_{DP}**-coated plates.

[†] Harvard Medical School.

[‡] Harvard University.

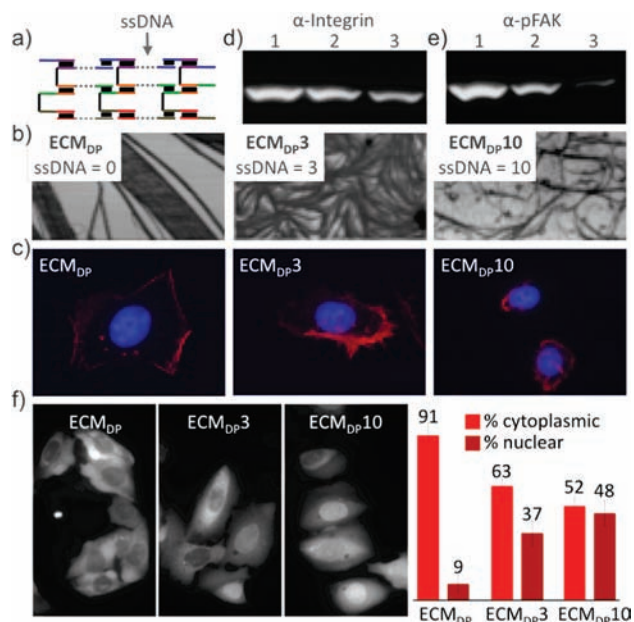


Figure 2. (a) Single-stranded domains are used to fine-tune the scaffold persistence length. (b) AFM analysis of (left to right) **ECM_{DP}**, **ECM_{DP3}**, and **ECM_{DP10}**. (c) Cell morphology as a function of single-stranded character: red, actin; blue, nucleus. (d) Relative amounts of integrin receptors bound to **ECM_{DP}**, **ECM_{DP3}**, and **ECM_{DP10}** (lanes 1–3, respectively). (e) Relative p-FAK expression levels as a function of **ECM_{DP}**, **ECM_{DP3}** and **ECM_{DP10}** (lanes 1–3, respectively). (f) GFP-FOXO1a localization as a function of scaffold persistence length; statistics are shown in the rightmost panel.

behavior.⁶ They were found to attach onto **ECM_{DP}**-coated glass plates with 96% efficiency (Scheme 1c and Figure 1c,d).⁵ Control experiments included the use of plates coated with **ECM_D**, **ECM_P**, unconjugated **ECM_D** and **ECM_P**, polylysine, and fibronectin.⁷ These controls revealed that HeLa cells were incapable of effectively adhering onto **ECM_D** or **ECM_P** unless they were assembled into **ECM_{DP}** and that **ECM_{DP}** was as effective as polylysine or fibronectin for cell adhesion (Figure 1d).⁵ The half-time of cell adhesion onto **ECM_{DP}** was 6 min, which was considerably shorter than their half-times for attachment onto polylysine or fibronectin (Figure 1e).⁵ The force of adhesion was determined as a measure of detachment. We pretreated cells with the protein synthesis inhibitor cycloheximide to prevent deposition of cell-derived ECM proteins. As shown in Figure 1f, 90% of the cells remained attached to **ECM_{DP}** when a detachment force of 780 pN was applied,⁵ which was considerably greater than the percentage of cells that remained attached to either polylysine or fibronectin. We also found that the effectiveness of **ECM_{DP}** was comparable to that of matrigel-coated surfaces.⁵ **ECM_{DP}** can thus be used as an effective ECM for cell seeding and attachment.

HeLa cells attached to **ECM_{DP}** remained viable and migrated. We conducted flow cytometry experiments on cells stained with the apoptosis and necrosis fluorophores Annexin-V-EGFP and 7-AAD.⁸ Only 4% of cells attached to **ECM_{DP}** stained positive for the apoptosis marker 48 h after adhesion, and none were necrotic (Figure 1g).⁵ In contrast, most of the cells attached to **ECM_D** died,⁵ indicating that the protein element of **ECM_{DP}** was essential for cell survival. Motility was determined using a modified Oris cell-migration assay. HeLa cells moved on **ECM_{DP}** at a rate of 46 $\mu\text{m}/\text{day}$ (Figure 1h), which was slightly higher than their rates on polylysine- or fibronectin-coated plates.⁵ **ECM_{DP}** thus promotes cell survival and migration.

The structure of the ECM influences the cell's cytoskeletal arrangement and shape.⁹ **ECM_{DP}** is fully double-stranded, and its persistence length (i.e., the length at which bending starts) is 1.2 μm .⁵ The incorporation of single-stranded domains should result in the formation of increasingly flexible assemblies that are structurally different (Figure 2a). **ECM_{DP3}** and **ECM_{DP10}** possess 3- and 10-base single-stranded regions and have persistence lengths of 0.95 and 0.32 μm , respectively (Figure 2b).⁵ **ECM_{DP3}** and **ECM_{DP10}** are thus structurally more flexible than the fully double-stranded **ECM_{DP}**. Importantly, HeLa cells growing on **ECM_{DP}**, **ECM_{DP3}**, and **ECM_{DP10}** were progressively more rounded (Figure 2c). These differences were confirmed by quantification of the substrate-bound integrin receptors (Figure 2d).⁵ Focal adhesions form in response to increasing ECM stiffness.⁸ Vinculin immunohistochemistry revealed a relative decrease in the number of assembled focal adhesions with increasing ECM flexibility.⁵ We confirmed that the observed differences in cellular behavior were due to the structural changes resulting from the use of single-stranded DNA domains by engineering a set of fully double-stranded DNA assembly analogues to **ECM_{DP}** in which the protein-to-protein distances were identical to those in **ECM_{DP3}** and **ECM_{DP10}**.⁵ Collectively, these results indicate that a profound cytoskeletal response can be achieved by controlling the substrate structure. On this basis, we proceeded to manipulate a number of integrin-mediated processes, such as the status of transduction proteins and the localization of intracellular transcription factors.

Focal adhesion kinase (FAK) is a signal transduction protein involved in cell development and migration and in the regulation of the tumor suppressor p53.¹¹ FAK is phosphorylated in response to focal adhesion formation¹¹ and thus can be fine-tuned as a function of ECM stiffness. As shown in Figure 2e, we were able to modulate the intracellular levels of p-FAK by modulating the degree of single-stranded character in the ECM.⁵

The integrin pathway can be used to activate cytoplasmic (vs nuclear) localization of the transcription factor FOXO1a.¹¹ To test whether ECM stiffness could be used to fine-tune the intracellular localization levels of FOXO1a, we engineered a stable human osteosarcoma U2OS cell line expressing GFP-tagged FOXO1a fusions.⁵ As shown in Figure 2f, by increasing the single-stranded character of the ECM, we were able to increase the nuclear levels of FOXO1a.⁵ We modulated FOXO1a localization, which has potential consequences for cell differentiation, proliferation, longevity, and apoptosis.¹⁰

In summary, we have constructed a new class of artificial extracellular matrices. Our approach involved the assembly of one-dimensional DNA ribbons decorated with cytoskeletal protein elements. We have demonstrated the potential of this material for ex vivo cellular scaffolding by showing that cells attach, survive, and grow and also demonstrated its capacity for structural programmability by fine-tuning cell morphology, cytoskeletal organization, signal transduction, and transcription factor localization. The diversity and addressability of DNA nanostructures suggests that a multitude of artificial ECMs could in principle be assembled using this approach. This contribution thus lays the groundwork for the modular construction of programmable ECMs for use in the systematic study and replication of the naturally occurring extracellular niche.

Acknowledgment. We thank the Wyss Institute for Biologically Inspired Engineering and the NIH (GM36373) for financial support. Microscopy data were acquired in the Nikon Imaging Center.

Supporting Information Available: Assembly of **ECM_{DP}**, **ECM_{DP3}**, and **ECM_{DP10}**; procedures and results of tissue-imaging, cell

attachment, cell viability, cell motility, and immunohistochemistry experiments; quantification of α -integrin and α -pFAK; and localization of FOXO1a. This material is available free of charge via the Internet at <http://pubs.acs.org>.

References

- (1) (a) Ikada, Y. *J. R. Soc., Interface* **2006**, *3*, 589–601. (b) Lutolf, M. P.; Hubbell, J. A. *Nat. Biotechnol.* **2005**, *23*, 47–55. (c) Griffith, L. G.; Naughton, G. *Science* **2002**, *295*, 1009–1014.
- (2) (a) Chan, B. P.; Leong, K. W. *Eur. Spine J.* **2008**, *17*, S467–S479. (b) Vasita, R.; Katti, D. S. *Int. J. Nanomed.* **2006**, *1*, 15–30. (c) Lee, K. Y.; Mooney, D. J. *Chem. Rev.* **2001**, *101*, 1869–1879.
- (3) (a) Lo, P. K.; Karam, P.; Aldaye, F. A.; McLaughlin, C. K.; Hamblin, G. D.; Cosa, G.; Sleiman, H. F. *Nat. Chem.* **2010**, *2*, 319–328. (b) Lin, C.; Liu, Y.; Yan, H. *Biochemistry* **2009**, *48*, 1663–1674. (c) Aldaye, F. A.; Palmer, A. L.; Sleiman, H. F. *Science* **2008**, *321*, 1795–1799. (d) Yin, P.; Hariadi, R. F.; Sahu, S.; Choi, H. M. T.; Park, S. H.; LaBean, T. H.; Reif, J. H. *Science* **2008**, *321*, 824–826. (e) He, Y.; Tian, Y.; Ribbe, A. E.; Mao, C. *J. Am. Chem. Soc.* **2006**, *128*, 15978–15979. (f) Um, S. H.; Lee, J. B.; Park, N.; Kwon, S. Y.; Umbach, C. C.; Luo, D. *Nat. Mater.* **2006**, *5*, 797–801.
- (4) Yamada, K. M. *Curr. Opin. Cell Biol.* **1989**, *1*, 956–963.
- (5) See the Supporting Information for details.
- (6) Masters, J. R. *Nat. Rev. Cancer* **2002**, *2*, 315–319.
- (7) We also conducted control experiments using unfunctionalized glass surfaces (see the Supporting Information for details).
- (8) 7-AAD also stains cells in late apoptosis. Thus, we were unable to determine the exact ratio of cell death caused by apoptosis vs necrosis, but given that only 4% of the cells died, we can conclude that **ECM_{DP}** is viable for cell growth.
- (9) (a) Discher, D. E.; Mooney, D. J.; Zandstra, P. W. *Science* **2009**, *324*, 1673–1677. (b) Discher, D. E.; Janmey, P.; Wang, Y.-L. *Science* **2005**, *310*, 1139–1143.
- (10) (a) Bershadsky, A. D.; Ballestrem, C.; Carramusa, L.; Zilberman, Y.; Gilquin, B.; Khochbin, S.; Alexandrova, A. Y.; Verkhovskiy, A. B.; Shemesh, T.; Kozlov, M. M. *Eur. J. Cell Bio.* **2006**, *85*, 165–173. (b) Wang, Y.-L. *Sci. Signaling* **2007**, *377*, 1–3.
- (11) (a) Hedrick, S. M. *Nat. Immunol.* **2009**, *10*, 1057–1063. (b) Maiese, K.; Chong, Z. Z.; Shang, Y. C.; Hou, J. *Med. Res. Rev.* **2009**, *29*, 395–418.

JA105431H